Analyst

Cite this: *Analyst*, 2012, **137**, 754

www.rsc.org/analyst

PAPER

Amperometric determination of xanthine in fish meat by zinc oxide nanoparticle/chitosan/multiwalled carbon nanotube/polyaniline composite film bound xanthine oxidase

Rooma Devi, Sandeep Yadav and C.S. Pundir*

Received 9th September 2011, Accepted 6th November 2011
DOI: 10.1039/c1an15838d

Xanthine oxidase (XOD) was immobilized on a composite film of zinc oxide nanoparticle/chitosan/carboxylated multiwalled carbon nanotube/polyaniline (ZnO-NP/CHIT/c-MWCNT/PANI) electrodeposited over the surface of a platinum (Pt) electrode. A xanthine biosensor was fabricated using XOD/ZnO-NP/CHIT/c-MWCNT/PANI/Pt as working electrode, Ag/AgCl as reference electrode and Pt wire as auxiliary electrode connected through a potentiostat. The ZnO-NPs were characterized by X-ray diffraction (XRD) and transmission electron microscopy (TEM), and the enzyme electrode was characterized by cyclic voltammetry, scanning electron microscopy (SEM), Fourier transform infrared (FTIR) spectroscopy and electrochemical impedance spectroscopy (EIS). The biosensor showed optimum response within 4 s at 0.5 V potential, pH 7.0, 35 °C and linear range 0.1–100 μM with a detection limit of 0.1 μM. The enzyme electrode was employed for determination of xanthine in fish meat during storage. The electrode lost 30% of its initial activity after 80 uses over one month, when stored at 4 °C.

Introduction

Xanthine oxidase, a molybdenum, iron and labile sulfur containing flavoprotein catalyzing the oxidation of hypoxanthine to xanthine and xanthine to uric acid, plays an important role in controlling purine metabolism.[1] Measurement of xanthine level in blood and tissue is very important for diagnosis and treatment of gout, xanthinuria and hyperuricaemia.[2] The determination of xanthine is also used in food industries for quality control of fish products. Hence, the quantification of xanthine is of clinical and industrial importance.[3–5] Several analytical methods such as colorimetry,[6] fluorometry,[7] HPLC,[8] mass spectrometry,[9] anion exchange chromatography, thin layer chromatography,[10] mass fragmentography,[11] and capillary column gas chromatography[12] have been reported for measurement of xanthine. Over the past few years, various electrochemical xanthine biosensors based on immobilized xanthine oxidase (XOD) have been reported.[13–16] However these XOD based biosensors have some common drawbacks such as poor stability, reusability, slow electron transfer, and complexity of immobilization. Therefore, there is a demand for the development of a biosensor that is comparatively more stable, reproducible and sensitive for xanthine determination in real samples.

Recently nanomaterials have been employed for improvement of analytical performance of biosensors.[16] Carbon nanotubes (CNTs), discovered in 1991 by Iijima,[17] represent an important group of nanoscale materials, because of special tube structure, good electrical conductivity, strong adsorptive ability, excellent bioconsistency, high electrocatalytic effect and a fast electron-transfer rate.[18,19] The addition of nanoparticles (NPs) of platinum, palladium, copper, nickel, ruthenium, silver, and gold onto the CNT films has generated new nanostructures with excellent behavior in the fields of optics, electronics, and electro-catalysis.[20–23] Integration of CNTs and some other materials such as conducting polymers, redox mediators and metal nanoparticles with a synergistic effect has shown particular promise as biochemical sensors.[23–25] Nanoparticle (NP) modified electrodes present unusual advantages in electroanalysis such as catalysis, enhancement of mass transport, high effective surface area and control over the electrode microenvironment.[26–28] Among the metal oxide nanoparticles, zinc oxide nanoparticles (ZnO-NPs) have been exploited as a potential material for biosensing, because of their unusual properties *i.e.* good biocompatibility, chemical stability, non-toxicity, high electron communication, high surface area for strong adsorption and high isoelectric point (IEP) (~9.5).[29] The excellent film-forming ability, good adhesion, biocompatibility, and high mechanical strength of CHIT membrane have made it a useful support for immobilization of biomolecules during the recent years.[30,31]

In the present study, we report the construction and application of a xanthine biosensor based on covalent immobilization of xanthine oxidase (XOD) on a ZnO-NP/CHIT/c-MWCNT/PANI composite film synthesized electrochemically on a platinum (Pt) electrode.

Department of Biochemistry, M D University, Rohtak, 124 001, India. E-mail: pundircs@rediffmail.com; Fax: +91 1262 295480; Tel: +91 9416492413

Experimental

Reagents and materials

Xanthine oxidase (XOD) (E.C.1.1.3.2) from buttermilk (0.15 U mg^{-1}), xanthine, and aniline (purified through vacuum distillation before use) were from SISCO Research Lab., Mumbai (India), chitosan was from Sigma-Aldrich, USA and carboxylated multiwalled carbon nanotubes (c-MWCNTs) were from Intelligent Materials Pvt. Ltd, Panchkula (Haryana), India. All other chemicals were of AR grade. Double distilled water (DW) was used in all experiments.

Instruments

An Autolab Potentiostat/Galvanostat (Eco Chemie, The Netherlands) was used for amperometric measurements as well as electrochemical impedance spectroscopic measurements (0.01–10^5 Hz). The size and morphology of ZnO-NPs was characterized by a transmission electron microscope (TEM) at the Department of Anatomy, All India Institute of Medical Sciences (AIIMS) New Delhi, X-ray diffraction (XRD) study of ZnO-NPs was carried out using a X-ray diffractometer (Rigaku,D/Max2550, Tokyo, Japan) at the Department of Physics, G.J. University, Hisar, collecting data in steps of 2-θ from 20 to 80 (2-θ) and morphological studies of the electrode were carried out with a scanning electron microscope (SEM) (Model Joel JSM-6510, Japan) at the Department of Chemistry, M.D. University, Rohtak. Fourier transform infrared (FTIR) spectra of the electrode were recorded using an FTIR spectrophotometer (Thermo Scientific, USA).

Construction of the XOD/ZnO-NP/CHIT/c-MWCNT/PANI/Pt electrode

Preparation of ZnO-NPs. ZnO-NPs were prepared as described[32] using a 0.45 M aqueous solution of zinc nitrate ($Zn(NO_3)_2 \cdot 4H_2O$) and 0.9 M aqueous solution of sodium hydroxide (NaOH). Zinc nitrate solution (50 mL) was added dropwise slowly for 40 min to the NaOH (100 mL) solution under high speed stirring. The beaker was sealed during this process for 2 h. The precipitated ZnO-NPs were washed with DW and ethanol and dried in air at 60 °C.

Preparation of the c-MWCNT/PANI/Pt electrode. One mg c-MWCNT was suspended in 1 ml mixture of concentrated H_2SO_4 and HNO_3 in 3 : 1 ratio and ultrasonicated for 2 h to get a finely dispersed black colored solution of c-MWCNTs and washed with DW. A solution for electrodeposition was prepared by adding aniline (50 μl) and finally dispersed c-MWCNT suspension (1 ml) into 1 N HCl (10 ml) in a glass cell. c-MWCNT/PANI was electrodeposited onto a Pt electrode through the cyclic voltammetry technique by applying 15 polymerization cycles at the potential range −0.2 to 0.8 V at a scan rate of 50 mV s^{-1}.[33] Prior to electrodeposition, the platinum electrode (1.85 cm × 1 mm) was polished with alumina slurry and then rinsed with DW. The resulting c-MWCNT/PANI/Pt modified electrode was washed thoroughly with DW.

Preparation of the ZnO-NP/CHIT/c-MWCNT/PANI/Pt electrode. CHIT (0.5 mg) flakes were dissolved in 10 mL of 0.05 M acetate buffer solution and kept overnight at room temperature. ZnO-NPs (5 mg) were dispersed into transparent CHIT solution and kept under magnetic stirring for about 30 min at room temperature followed by sonication for about 1 h. The hybrid composite film of ZnO-NP/CHIT solution was electrodeposited on the c-MWCNT/PANI/Pt electrode by cyclic voltammetry using the potential range −0.2 to 0.9 V at a scan rate of 50 mV s^{-1}. The ZnO-NP/CHIT/c-MWCNT/PANI/Pt electrode was washed with DW followed by 50 mM phosphate buffer (PB), pH 7.0 and allowed to dry at room temperature.

Immobilization of XOD onto the ZnO-NP/CHIT/c-MWCNT/PANI/Pt electrode

The XOD was immobilized onto the ZnO-NP/CHIT/c-MWCNT/PANI/Pt electrode surface by a covalent bond (C═N bond) between NH_2 of the enzyme and the –CHO group of glutaraldehyde. A 100 μL of XOD was added to 10 mL 2.5% glutaraldehyde and then 6 μL of the composite solution was dropped on the surface of the ZnO-NP/CHIT/c-MWCNT/PANI/Pt electrode. The resulting enzyme electrode was dried and then stored in a refrigerator at 4 °C, when not in use. The fabricated electrode was characterized by cyclic voltammetry, SEM, FTIR spectroscopy and EIS studies.

Optimization of the XOD/ZnO-NP/CHIT/c-MWCNT/PANI/Pt electrode

To determine the optimum working conditions of the enzyme electrode, the pH of reaction buffer (50 mM) was varied from pH 3.0–8.0 at an interval of pH 0.5 using acetate buffer in the pH range 3.0–5.0 and PB in the pH range 6.0–8.0. Similarly, to determine optimum temperature, the reaction mixture was incubated at 15–55 °C at an interval of 5 °C. To determine the optimum response time, the current response was studied from 1–40 s. To study the effect of substrate concentration, different xanthine concentrations, ranging from 0.1–600 μM, were used (Fig. 1A).

Xanthine determination in fish meat

Labeo fish was purchased from a local market. The fish was chopped and homogenized in 5 mL 0.5 M $HClO_4$ until a fine paste was obtained for the precipitation of proteins. The denatured sample was stirred mechanically for 10 min and then centrifuged at 4000 rpm for 5 min. The supernatant was collected, its pH was adjusted to 7.0 with NaOH, and it was diluted 10 times. This fish meat extract was then divided into two parts. One part was used immediately and the other was stored at room temperature for storage studies.[16] To determine xanthine content in fish meat extract, the same procedure was used as described for sensor response measurement under the optimal working conditions except that xanthine was replaced by the fish meat extract. The xanthine content in the fish meat extract was interpolated from the standard curve between xanthine concentrations *vs.* current (mA) prepared under optimal working conditions (Fig. 1B and C).

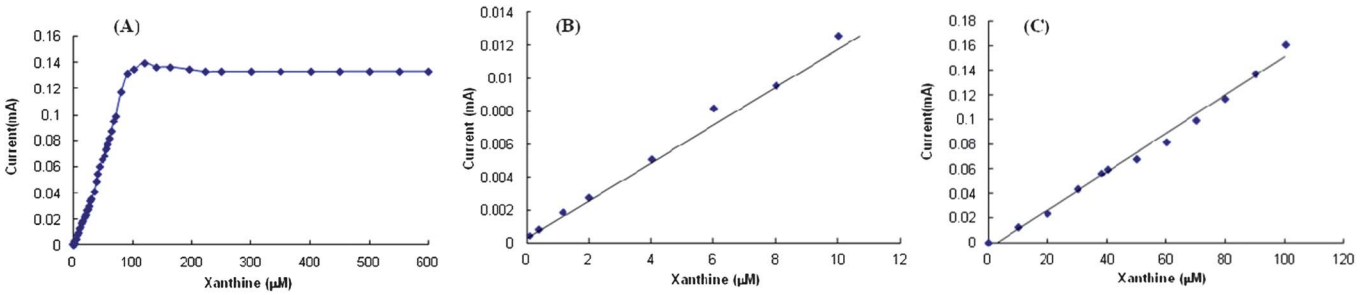

Fig. 1 Effect of xanthine concentration on response of the xanthine biosensor (A) and the standard curve of xanthine at lower concentration range (B) and at higher concentration range (C) showing the linear relationship by the xanthine biosensor based on the XOD/ZnO-NP/CHIT/c-MWCNT/PANI/Pt electrode.

Evaluation

The performance of this biosensor was evaluated for linearity, detection limit, analytical recovery, precision and accuracy.

Results and discussion

Characterization of ZnO-NPs

The characterization of ZnO-NPs was carried out by TEM. Samples of ZnO-NPs were milled together with anhydrous alcohol and then dispersed in anhydrous alcohol to form a dilute suspension. The dilute suspension was dropped on the carbon-grid and the morphology of the ZnO-NPs was observed using TEM (Fig. 2A). The morphology of ZnO was crystallite rather than spherical. The diameter of ZnO nanoparticle sizes was 10–30 nm. The structure of ZnO-NPs was also characterized by XRD (Fig. 2B). All peaks were consistent with the peaks of ZnO-NPs with high crystallinity. The X-ray diffraction data were recorded using Cu Kα radiation (1.5406 Å). The intensity data were collected over a 2θ range of 20–80°. A definite line broadening of the diffraction peaks is an indication that the synthesized materials are in the nanometre range. The grain size was found to be in the range of 7–24 nm depending on the growth condition. The lattice parameters calculated were also in agreement with the reported values.

Construction of the XOD/ZnO-NP/CHIT/c-MWCNT/PANI/Pt electrode

The fabrication of the xanthine biosensor based on the XOD/ZnO-NP/CHIT/c-MWCNT/PANI/Pt modified electrode is summarized in Fig. 3. Firstly the c-MWCNT/PANI composite film was deposited on the Pt electrode using cyclic voltammetry. Then, the ZnO-NP/CHIT film is electrochemically deposited on the surface of the c-MWCNT/PANI composite film. The ZnO-NP/CHIT/c-MWCNT/PANI composite film exhibits higher currents than the c-MWCNT/PANI composite film (Fig. 4A), which indicates that the ZnO-NP/CHIT/c-MWCNT/PANI composite film has a larger effective surface area than the c-MWCNT/PANI composite film and the ZnO-NP/CHIT/c-MWCNT/PANI composite film could provide conducting path through the composite matrix for faster kinetics. XOD, when treated with glutaraldehyde solution, leads to formation of a covalent bond (C=N bond) between NH_2 of the enzyme and the –CHO group of glutaraldehyde. This pretreated enzyme, when applied onto the ZnO-NP/CHIT/c-MWCNT/PANI/Pt electrode, leads to formation of another covalent bond (C=N bond) between NH_2 of chitosan and the –CHO group of glutaraldehyde.

To evaluate the catalytic activity of the XOD/ZnO-NP/CHIT/c-MWCNT/PANI/Pt electrode, the modified electrode was characterized by a cyclic voltammogram in the presence of xanthine in the potential range from −0.1 V to +0.8 V. Fig. 4B shows the cyclic voltammogram of the XOD/ZnO-NP/CHIT/c-MWCNT/PANI/Pt electrode in 50 mM PB (pH 7.0) with xanthine (0.1–100 μM) solution. The electrochemical reactions involved in response measurement of the xanthine biosensor are given below:

$$\text{Xanthine} + O_2 + H_2O \xrightarrow{\text{XOD on hybrid film}} \text{Uric acid} + H_2O_2$$

$$H_2O_2 \xrightarrow{0.5\ \text{V}} 2H^+ + 2e^- + O_2$$

$$2e^- \longrightarrow \text{Pt electrode}$$

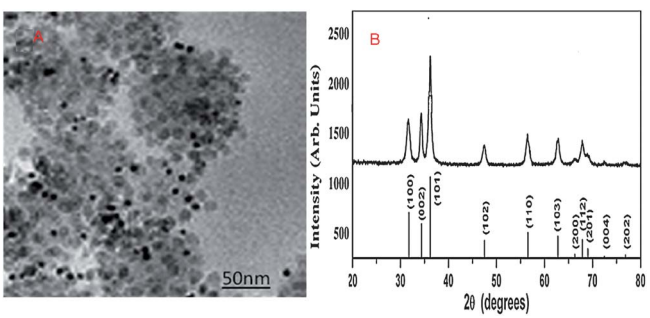

Fig. 2 (A) Transmission electron microscopic (TEM) images of ZnO-NPs and (B) the X-ray diffraction (XRD) pattern of ZnO-NPs.

Surface characterization using SEM

The morphology of the c-MWCNT/PANI/Pt electrode, ZnO-NP/CHIT/c-MWCNT/PANI/Pt electrode and XOD/ZnO-NP/CHIT/c-MWCNT/PANI/Pt electrode was characterized by SEM studies. SEM images show a layer of the c-MWCNT/PANI/Pt electrode (Fig. 5A), the presence of ZnO-NPs on the c-MWCNT/PANI/Pt electrode in cluster forms (Fig.5B), and the globular structure indicating the presence of immobilized XOD (Fig. 5C) on the nanocomposite hybrid electrode.

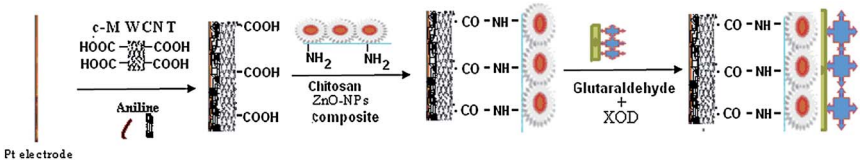

Fig. 3 Schematic representation of chemical reactions involved in fabrication of the XOD/ZnO-NP/CHIT/c-MWCNT/PANI/Pt electrode.

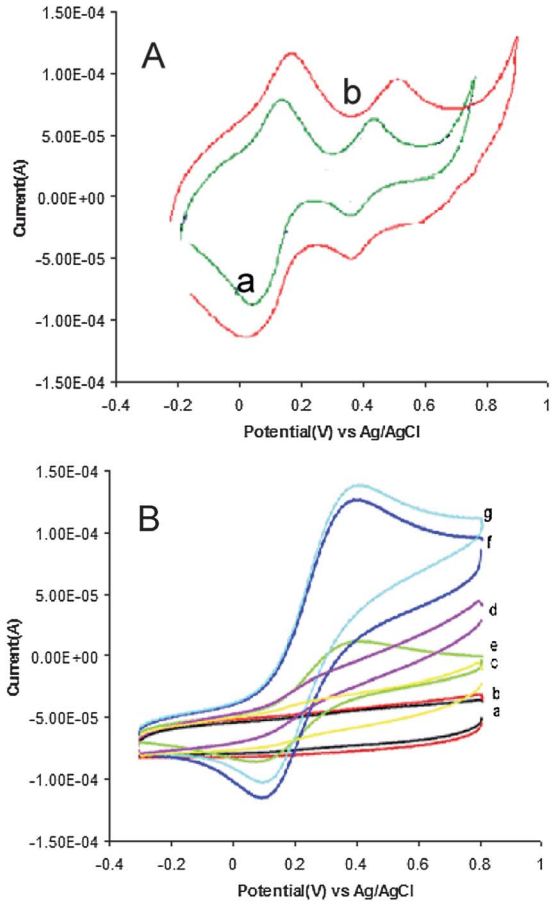

Fig. 4 Cyclic voltammogram for electrochemical deposition of (A) the (a) c-MWCNT/PANI/Pt electrode and (b) ZnO-NP/CHIT/c-MWCNT/PANI/Pt electrode. (B) Cyclic voltammetry of amperometric response studies of the XOD/ZnO-NP/CHIT/c-MWCNT/PANI/Pt electrode in xanthine concentration from $a = 0.1$ to $g = 100$ μM using a phosphate buffer (50 mM, pH 7.0).

FTIR spectra

FTIR spectra of the c-MWCNT/PANI/Pt electrode (Fig. 6A) showed bands at 1460 and 1604 cm^{-1} which are caused by benzoid and quinoid vibrations. The presence of peaks at 1138 and 3420 cm^{-1} is attributed to β-N^{+}=Q and –N–H stretching vibrations of PANI in the composite. The FTIR spectrum of the ZnO-NP/CHIT/c-MWCNT/PANI/Pt electrode (Fig. 6B) showed an additional peak at 492 cm^{-1} due to ZnO-NPs and a broad peak at 3418 cm^{-1} due to characteristic absorption bands of amino saccharide in chitosan due to overlapping of –OH and $–NH_2$ stretching. The peaks at 1065 and 1140 cm^{-1} become deeper due to C–N bonding between CHIT and c-MWCNT. The FTIR spectrum of the XOD/ZnO-NP/CHIT/c-MWCNT/PANI/Pt (Fig. 6C) electrode showed characteristic peaks at 1647 and 1495 cm^{-1} attributed to the primary and secondary amide linkages of enzyme molecules, which confirmed the presence of C=N bond.

Electrochemical impedance measurements

The charge transfer process in the XOD/ZnO-NP/CHIT/c-MWCNT/PANI/Pt electrode was studied by monitoring charge transfer resistance (R_{CT}) at the electrode and electrolyte interface. The value of the R_{CT} depends on the dielectric and insulating features at the electrode/electrolyte interface. Fig. 7 shows electrochemical impedance spectra (EIS) of the (a) c-MWCNT/PANI/Pt electrode, (b) ZnO-NP/CHIT/c-MWCNT/PANI/Pt electrode and (c) XOD/ZnO-NP/CHIT/c-MWCNT/PANI/Pt electrode in 5 mM $K_3Fe(CN)_6/K_4Fe(CN)_6$ (1 : 1) containing 0.05 M PB, pH 7.5. The R_{CT} values for the c-MWCNT/PANI/Pt electrode, ZnO-NP/CHIT/c-MWCNT/PANI/Pt electrode and XOD/ZnO-NP/CHIT/c-MWCNT/PANI/Pt electrode were 1.5320 Ω, 1.412 Ω and 8.645 Ω respectively. It was observed that the R_{CT} of the ZnO–NP/CHIT/c-MWCNT/PANI/Pt modified electrode (curve b) is lower than that of the c-MWCNT/PANI/Pt modified electrode (curve a). The results show that the ZnO-NP/CHIT/c-MWCNT/PANI/Pt modified electrode decreases the resistance of the electrode and holds high electron transfer efficiency, while the R_{CT} of the XOD/ZnO-NP/CHIT/c-MWCNT/PANI/Pt electrode (curve c) increases over that of the ZnO-NP/CHIT/c-MWCNT/PANI/Pt modified electrode. This increase in R_{CT} is attributed to the fact that most biological molecules, including enzymes, are poor electrical conductors at low frequencies and cause hindrance to electron transfer. These

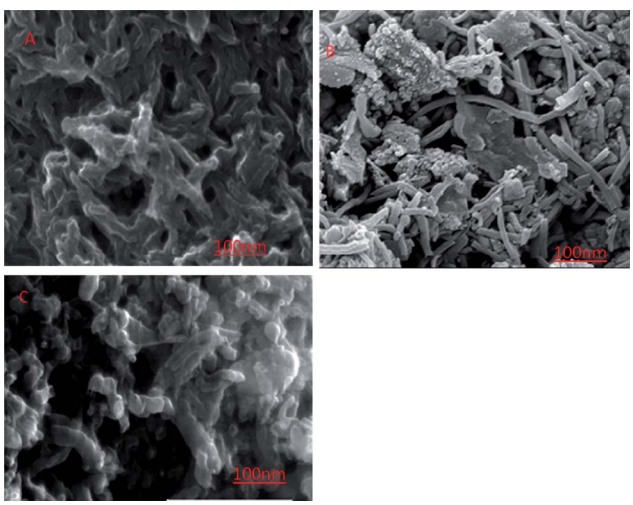

Fig. 5 SEM images of (A) c-MWCNT/PANI/Pt, (B) ZnO-NP/CHIT/c-MWCNT/PANI/Pt and (C) XOD/ZnO-NP/CHIT/c-MWCNT/PANI/Pt electrodes.

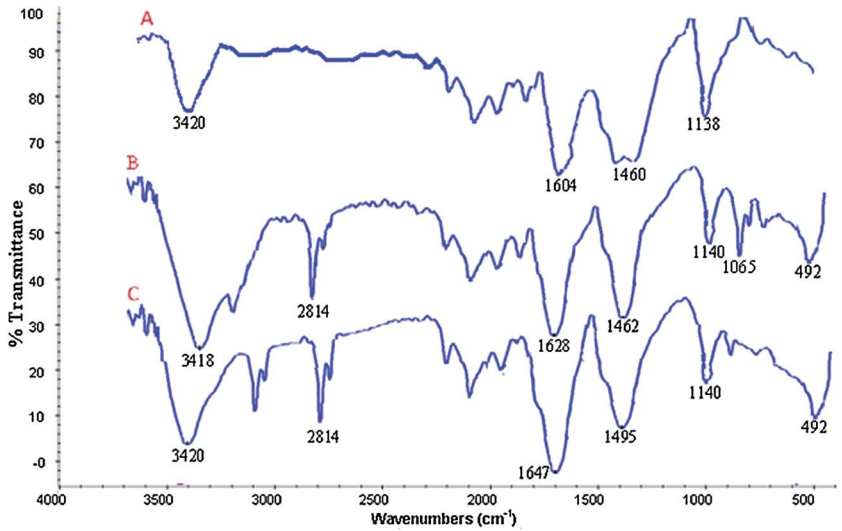

Fig. 6 FTIR spectra of (A) c-MWCNT/PANI/Pt, (B) ZnO-NP/CHIT/c-MWCNT/PANI/Pt and (C) XOD/ZnO-NP/CHIT/c-MWCNT/PANI/Pt electrodes.

results also indicate binding of XOD onto the ZnO-NP/CHIT/c-MWCNT/PANI/Pt electrode.

Optimization of experimental conditions

The experimental conditions affecting the biosensor response were studied in terms of effect of pH, incubation temperature, time and substrate (xanthine) concentration. The optimum current was obtained within 4 s at pH 7 and 35 °C. There was a hyperbolic relationship between the biosensor response and xanthine concentration up to a final concentration of 100 μM, after which it was constant (Fig. 1A).

Evaluation of the xanthine biosensor

There was a linear relationship between the xanthine concentration ranging from 0.1–100 μM and current (mA), which is better than the earlier xanthine biosensors based on a modified graphite electrode coated with gelatin (upto 40 μM),[34] carbon nanotube (CNT) modified carbon paste electrode (1–100 μM)[35] and zinc oxide nanoparticle–polypyrrole composite film (0.8–40 μM).[16] The detection limit of the biosensor was 0.1 μM ($S/N = 3$), which is lower than that of the modified graphite electrode coated with gelatin (4.5 μM),[34] modified carbon paste electrode (1 μM),[35] polypyrrole modified film (400 μM),[36] FeTPP-NP modified glassy carbon (1 μM)[37] and zinc oxide nanoparticle–polypyrrole composite film (0.8 μM).[16] Analytical recoveries of exogenously added xanthine in fish extract (10 mg l^{-1}, 20 mg l^{-1}) by the present method were 95.1% and 96.1%, respectively, showing the reliability of the method. Within and between batch coefficients of variation (CV) in xanthine concentration in fish extract after one week of storage at −20 °C were <5.2% and <5.30%, showing the good reproducibility and reliability of the method. To know the accuracy of the present method, values of xanthine in fish meat sample were determined by the enzymic colorimetric method and by the present method. The xanthine values obtained by the present biosensor matched with those by the enzymic colorimetric method with a good correlation (r = 0.93, significant at 1% level).

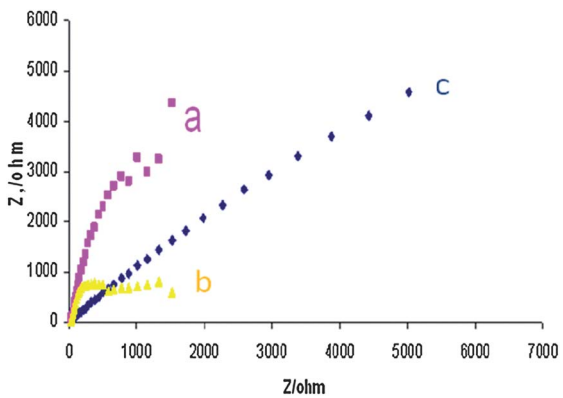

Fig. 7 Impedance spectra of the (a) c-MWCNT/PANI/Pt electrode, (b) ZnO-NP/CHIT/c-MWCNT/PANI/Pt electrode and (c) XOD/ZnO-NP/CHIT/c-MWCNT/PANI/Pt electrode in phosphate buffer (50 mM, pH 7.0), containing $[K_3Fe(CN)_6]/[K_4Fe(CN)_6]$ (5 mM).

Effect of interfering compounds

The ability of the immobilized enzyme layer to protect the sensor from electroactive interference was investigated. Other coexisting substances found in meat sample were studied for any possible interfering effect on analysis of xanthine in meat sample. A known concentration (40 μM) of inosine 5-phosphate (IMP), inosine, cystine, uric acid, caffeine, theophylline, hypoxanthine and ascorbic acid was added to 0.15 mM xanthine solution. It has been shown that inosine 5-phosphate (IMP), inosine, cystine, caffeine, theophylline and uric acid have no interfering effects on analysis of xanthine but ascorbic acid (20%) and hypoxanthine (30%) interfere in the analysis of xanthine.

Xanthine determination in fish meat

The xanthine concentration in fish meat was determined during its 16 days of storage at room temperature by using the present

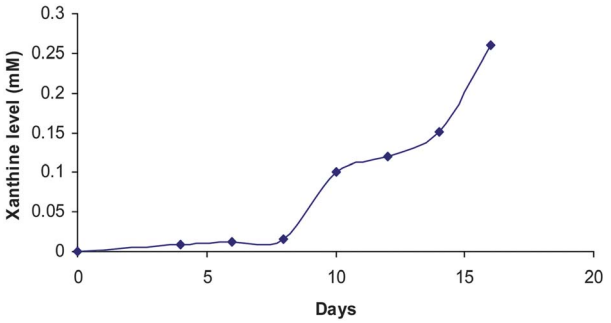

Fig. 8 Determination of xanthine in fish meat by the xanthine biosensor based on the XOD/ZnO-NP/CHIT/c-MWCNT/PANI/Pt electrode during storage at room temperature (30 ± 5 °C).

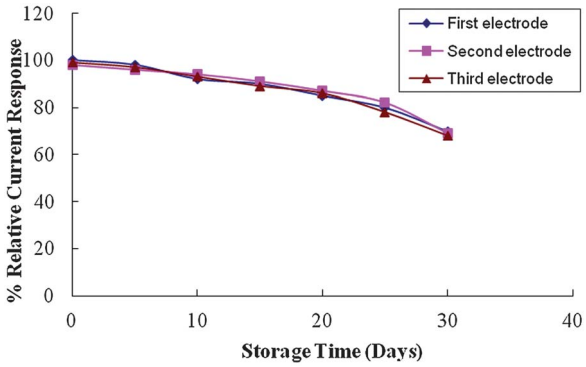

Fig. 9 Effect of storage at 4 °C on response of three similar XOD/ZnO-NP/CHIT/c-MWCNT/PANI/Pt electrodes.

biosensor. The xanthine level was increased with the storage time. It was double on day 10, compared to that on day 1 (Fig. 8).

Long-term stability of the electrode

To examine the long-term storage stabilities, the activity of the XOD/ZnO-NP/CHIT/c-MWCNT/PANI/Pt electrode was tested with respect to storage time. The enzyme electrode was constructed thrice and the effect of storage at 4 °C was studied on the response of these three similarly constructed electrodes. The results showed practically no variation in storage stability of the three electrodes. The electrode lost only 30% of its initial activity after its 80 regular uses over 1 month (Fig. 9).

Conclusion

An improved amperometric xanthine biosensor was constructed by immobilizing XOD onto a ZnO-NP/CHIT/c-MWCNT/PANI modified Pt electrode. The biosensor showed better sensitivity, wider working range and longer storage stability.

References

1 R. Hille, *Arch. Biochem. Biophys.*, 2005, **433**, 107–116.
2 X. Liu, W. M. Lin, X. H. Yan, X. H. Chen, J. R. Hoidal and P. Xu, *J. Chromatogr., B: Biomed. Sci. Appl.*, 1998, **785**, 101–114.
3 R. Harrison, *Free Radical Biol. Med.*, 2002, **33**, 774–797.
4 D. Shan, Y. Wang, M. Zhu, H. Xue, S. Cosnier and C. Wang, *Biosens. Bioelectron.*, 2009, **24**, 1171–1176.
5 D. Shan, Y. Wang, H. Xue and S. Cosnier, *Sens. Actuators, B*, 2009, **136**, 510–515.
6 G. Berti, P. Fossati, G. Tarenghi, C. Musitelli and G. V. Melzideril, *J. Clin. Chem. Clin. Biochem.*, 1988, **26**, 399–404.
7 J. S. Beckman, D. A. Parks, J. D. Pearson, P. A. Marshall and B. A. Freeman, *Free Radical Biol. Med.*, 1989, **6**, 607–615.
8 R. Kock, B. Delvoux and H. Gresiling, *J. Clin. Chem. Clin. Biochem.*, 1993, **31**, 303–310.
9 R. Prker, W. Snedden and R. W. Watts, *Biochem. J.*, 1969, **115**, 103–108.
10 H. S. Nakatani, L. V. D. Santos, C. P. Pelegrine, M. Gomes, M. Matsushita, N. E. D. Souza and J. V. Visentainer, *Am. J. Biochem. Biotechnol.*, 2005, **1**, 85–89.
11 R. O. Olojoa, R. H. Xiab and J. J. Abramsona, *Anal. Biochem.*, 2005, **339**, 338–344.
12 S. Renata, L. Pagliarussi, A. P. Luís, L. Freitas and J. K. Bastos, *J. Sep. Sci.*, 2002, **25**, 371–374.
13 J. Pei and X. Y. Li, *Anal. Chim. Acta*, 2000, **414**, 205–213.
14 Y. Lui, N. Lo, W. Tao and S. Yao, *Electroanalysis*, 2004, **16**, 1271–1278.
15 R. Devi, J. Narang, S. Yadav and C. S. Pundir, *J. Anal. Chem.*, in press.
16 R. Devi, M. Thakur and C. S. Pundir, *Biosens. Bioelectron.*, 2011, **26**, 3420–3426.
17 S. Iijima, Helical microtubules of graphite carbon, *Nature*, 1991, **354**, 56–58.
18 F. Zhang, X. Wang, S. Ai, Z. Sun, Q. Wan, Z. Zhub, Y. Xian, L. Jin and K. Yamamoto, *Anal. Chim. Acta*, 2004, **519**, 155–161.
19 Y. Lin, R. X. Wang and X. M. Li, *Electrochem. Commun.*, 2005, **7**, 597–601.
20 A. Hussain, M. A. Kabir and A. K. Sood, *Curr. Sci.*, 2009, **96**, 664–673.
21 L. Wang, S. J. Guo, L. J. Huang and S. J. Dong, *Electrochem. Commun.*, 2007, **9**, 827–832.
22 J. S. Ye, Y. C. Bai and W. D. Zhang, *Microchim. Acta*, 2009, **165**, 361–366.
23 C. L. Xu, J. F. Chen, Y. Cui, Q. Y. Han, H. Choo, P. K. Liaw and D. H. Wu, *Adv. Eng. Mater.*, 2006, **8**, 73–77.
24 M. H. Yang, Y. H. Yang, Y. L. Liu, G. L. Shen and R. Q. Yu, *Biosens. Bioelectron.*, 2006, **21**, 1125–1136.
25 Y. J. Zou, C. L. Xiang, L. X. Sun and F. Xu, *Biosens. Bioelectron.*, 2008, **23**, 1010–1016.
26 X. L. Luo, J. J. Xu, Y. Du and H. Y. Chen, *Anal. Biochem.*, 2004, **334**, 284–289.
27 C. M. Welch and R. G. Compton, *Anal. Bioanal. Chem.*, 2006, **384**, 601–605.
28 S. P. Singh, S. K. Arya, M. K. Pandey, B. D. Malhotra, S. Saha, K. Sreenivas and V. Gupta, *Appl. Phys. Lett.*, 2007, **91**, 63901–63903.
29 Y. J. Zhang, Y. Wen, Y. Liu, D. Li and J. H. Li, *Electrochem. Commun.*, 2004, **6**, 1180–1184.
30 S. Hikima, T. Kakizaki, M. Taga, K. Hasebe and J. Fresenius, *Anal. Chem.*, 1993, **45**, 607–610.
31 L. Chen and W. Gorski, *Anal. Chem.*, 2001, **73**, 2862–2868.
32 Y. J. Zou, C. L. Xiang, L. X. Sun and F. Xu, *Biosens. Bioelectron.*, 2008, **23**, 1010–1016.
33 A. B. Moghaddam, T. J. Badraghi and M. Kazemzad, *Int. J. Electrochem. Sci.*, 2009, **4**, 247–257.
34 N. Dimcheva, E. Horozova and Z. Jordanova, *Anal. Chim. Acta*, 2002, **57**, 883–889.
35 U. Anik and M. Cubukc, *Turk. J. Chem.*, 2008, **32**, 711–719.
36 F. Arslan, A. Yasar and E. Kilic, *Artif. Cells, Blood Substitutes, Biotechnol.*, 2006, **34**, 113–128.
37 X. H. Li, Z. H. Xie, H. Min, Y. Z. Xian and L. Tongjin, *Anal. Lett.*, 2008, **41**, 456–468.